FACTA UNIVERSITATIS
Series: **Mechanical Engineering**
https://doi.org/10.22190/FUME220127030M

Original scientific paper

EFFECT OF ELECTRIC PULSING ON THE STRUCTURE, TEXTURE AND HARDNESS OF CRYOROLLED FINE-GRAIN COPPER

Mikhail Markushev, Irshat Valeev, Aygul Valeeva, Rafis Ilyasov, Elena Avtokratova, Stanislav Krymskiy, Oleg Sitdikov

Institute for Metals Superplasticity Problems, Russian Academy of Sciences, Ufa, Russia

Abstract. *A synergy effect of cryorolling and high-dense electric pulsing on the structure, texture and hardness of fine-grain Cu is analyzed. More than twice Cu strengthening under rolling with 90% reduction at –196°C was caused by strong rolling texture and work-hardened nanostructure with ~300 nm crystallites and ~30% fraction of high-angle boundaries. Further single pulsing with current intensity K_j = 3.5×10^4 A^2s/mm^4 resulted in a static recovery and slight Cu softening due to the formation of a more equilibrium structure with lower dislocation density and lattice microstrain. Increasing K_j to 3.8×10^4 A^2s/mm^4 led to a sharp drop in the Cu hardness owing to continuous recrystallization and texture randomization. At K_j near 5.0×10^4 A^2s/mm^4 homogeneous ultrafine-grain structure with 1 μm defect free equiaxed grains and about 30% of twin boundaries is formed. Normal grain growth to 3 μm and gradual decrease of the Cu hardness were taking place at higher pulsing energies, up to 8.1×10^4 A^2s/mm^4.*

Key Words: *Copper, Cryorolling, Electric Pulsing, Structure, Texture, Hardness*

1. INTRODUCTION

One of the promising but still quite poorly studied methods of processing ultrafine-grained (UFG) (with a grain size less than 1 μm) metals and alloys is the so-called cryogenic deformation, which is carried out at temperatures below 120K (-153°C) [1]. It is well known that lowering the deformation temperature leads to the materials strengthening due to the suppression of dynamic recovery and accumulation of internal stresses, mainly owing to the increase in densities of crystal defects. One of the basic results of such structure changes is intensification of dynamic and static grain refinement under straining [2-5] and subsequent thermal [2,6] or other energy action [7-9]. However,

*Received: January 27, 2022 / Accepted July 15, 2022
Corresponding author: Mikhail Markushev
Institute for Metals Superplasticity Problems RAS, 39 Khalturin St., Ufa, 450001, Russia
E-mail: mvmark@imsp.ru

a number of data published have declared that cryogenic deformation, even using methods of the severe plastic deformation (SPD) with strains of $e>1$, does not guarantee the UFG structure formation. For instance, it was found [10] that the SPD, realized by cryorolling (CR), did not result in the expected UFG structure development and even the significant grain refinement in pure aluminum. Similar behavior has been also found in copper and brass [11, 12], being conditioned by suppressing the dislocation double cross slip with temperature decrease. The latter, in turn, complicated the formation of strain-induced boundaries and grain fragmentation (subdivision) and thus restricted the development of new grains by dynamic recrystallization. Nevertheless, the authors of [13-17] concluded that a complex thermomechanical treatment (TMT), involving cryorolling and subsequent high-dense electric pulsing (HDEP) [18, 19], ensured the UFG sheet production. It should be noted that under such a treatment the regimes of pulsing played a dominant role in intensity and completeness of static recovery and recrystallization of a preliminary highly work-hardened material, allowing grain refinement due to the extremely fast heating and short time thermal action at HDEP. Another critical point is the effect of the initial (before CR) state on the structure development in the processing material. For instance, in [13] the HDEP following cryorolling was shown as successful technology to process Cu sheets with near homogeneous UFG structure. However, the result was obtained for the preliminary severely forged UFG billet [20]. In that case, the processing was narrowed to a quite simple task – to preserve the processed UFG structure during further CR and HDEP. So, the crucial point is to analyze the ability of Cu with coarser grains to form UFG structure under the similar TMT mode.

Thus, the aim of the present investigation was to evaluate the potential of TMT, basing on cryorolling as the only solo SPD technique in combination with powerful single electric pulsing, and to study the effect of HDEP energy on structuring and hardening/softening of pure copper with initial fine-grain structure.

2. MATERIAL AND METHODS

The ingot out of pure copper (designated as M1 in accordance with the Russian standard GOST 859-2001) was preliminary isothermally forged at 850°C and further annealed at 500°C for 2 hrs to process recrystallized fine-grain structure with 10-15 μm grain size [21]. Subsequent SPD *via* rolling with reduction of about 5% per pass of mechanically cut out plates was carried out to a total strain of about 90% (e=2.3) at –196°C using six-roll mill. Isothermal conditions of straining were obtained by the preliminary 1 hr holding of the billets and removable working rolls in liquid nitrogen. Further HDEP (see more details in [13-16]) was carried out on the dog-bone samples with 3×4 mm^2 gage part, cut out from 0.4 mm thick sheets along their rolling direction. For the used integral current density (K_j) from 3.5×10^4 to 8.1×10^4 A^2s/mm^4, the calculated temperature of gage heating (T_c) was within the range of 260-900°C. With the impulse time of about 10^{-4} s and the current frequency of 10^4 Hz, the depth of its penetration inside the sample was about 0.92 mm. This means the absence of the skin-effect under HDEP, suggesting a uniform current distribution in the cross-section of a sample.

For distinct characterization of structures under TMT the scanning electron microscope "TESCAN MIRA 3 LMH" equipped with "HKL Channel 5" software was used. As was recommended in [22, 23] the EBSD data and maps were obtained from 6 Kikuchi-line scanning in the rolling plane with two steps of 100 and 500 nm. Grain boundary misorientation angle of 15° was taken as criterion for division into low- and high-angle boundaries (LABs and HABs). The mean subgrain and grain sizes (d and D, consequently) were determined as equivalent diameter of not less than 900 crystallites. The average angle of misorientation (Θ) and fraction of HABs and twin boundaries (Σ3 and Σ9) (F_{HAB} and F_{Σ}, consequently) were determined for boundaries with misorientation angle higher than 2°. The fraction of recrystallized grains (F_{rec}) was calculated as the ratio of the areas of recrystallized grains (with internal lattice distortion less than 2°) and the whole scanning area. Pole figures and texture components were derived from 500 nm scanning of not less than 2000 crystallites [22] with an angular deviation of 15°.

X-ray diffractometry (XRD) was carried out on a DRON-4-07 in Cu-K_{α} radiation at a voltage of 40 kV and a current of 30 mA with a wavelength of λ = 1.54418 Å, and a graphite monochromator on a diffracted beam. The scanning step of 0.1° and an exposure time of 4 s with rotation of the sample were used. The root-mean-square microstrain of the copper lattice ($<\varepsilon^2>^{1/2}$), as well as the coherent domain size (D), were determined by the full-profile method in the MAUD software. The dislocation density (ρ) was found as $\rho=2\sqrt{3}<\varepsilon^2>^{1/2}/Db$, where b is the Burgers vector.

Strength of the copper was characterized by the Vickers microhardness, estimated from not less than ten measurements per point on the MVDM 8 "AFFRY" tester at 0.5N force and the loading time of 10 s.

If not mentioned, the error of measurements of any parameter did not exceed 5%.

3. Results and Discussions

Four characteristic intervals on the Cu hardness dependence *vs.* the regimes of the TMT studied were clearly distinguished (Fig. 1). The first one (I) derived from the copper multiple strengthening due to cryorolling. In the second range (II), lasting to HDEP with low energies, hardness changed scarcely, indicating the interval of pulsing where the deformation structure was quite stable. The third (III) stage started from some "threshold" level of current density (about 3.5×10^4 A^2s/mm^4) and occupied an extremely narrow range of pulsing energy, resulting in a sharp drop in Cu hardness. And in the fourth one (IV) (at $K_j > 3.8\times10^4$ A^2s/mm^4), there was a final and less intense softening of the strained metal down to the level close to the starting fine-grain annealed condition.

Judging by the data in Figs. 1 and 2, and Tabs. 1 and 2, the HDEP with the minimum energy of 3.5×10^4 A^2s/mm^4 did not cause any significant changes in the linear parameters of the structure, hardness and the lattice parameter of as-rolled copper. The structure still remained partially recrystallized deformation-like one with well-developed nanosized (sub)grains (Figs. 2a-d). It should be noted that in distinction with the data published in [21], the present measurements obtained with less step of scanning, gave significantly reasonable data, regarding, first of all, the grain and subgrain sizes (Tab. 1). Simultaneously, HDEP led to sense decrease in the coherent domain size and enhancement of angular parameters, involving fractions of HABs and recrystallized grains (Tabs. 1 and 2). It was also accompanied by more than 50% reductions of the

micro-stresses and the dislocation densities. Obviously, the structure transformations found indicated an occurrence of static recovery and recrystallization *in-situ*, which, along with a noticeable increase in the structure equilibrity and homogeneity, supposed the significant Cu softening. Thus, the absence of a noticeable loss of hardness can only be attributed to structural strengthening due to transformations of the deformation-induced dislocation boundaries into more equilibrium (sub)grain ones. Virtually, such changes have to result in Cu hardening, which turned out to be sufficient to compensate softening caused by a reduction in the lattice defectiveness.

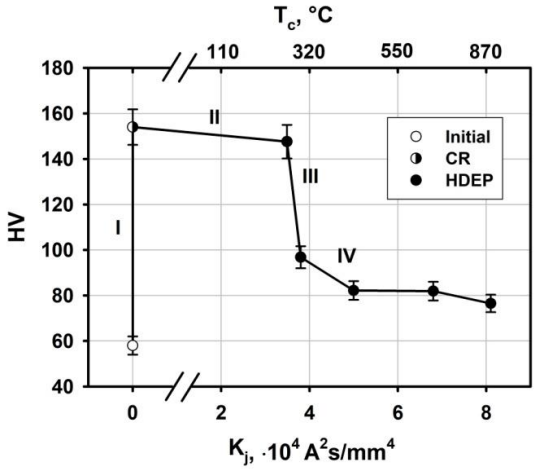

Fig. 1 Cu hardness (HV) changes due to cryorolling (CR) and energy of high-dense electric pulsing (HDEP) (bottom scale) / corresponding temperature (T_c) (upper scale)

When the current density reached 3.8×10^4 A^2s/mm^4, the stored deformation energy (and hardness, consequently (Fig. 1)) are sharply reduced, owing to the development of a statically recrystallized UFG structure (Fig. 2e,f) with a significantly higher subgrain-, grain- and coherent domain size (Tabs. 1 and 2). The structure was also characterized by almost complete relaxation of lattice micro-stresses due to recrystallization [24] and a drastic decrease in dislocation density to equilibrium level (Tab. 2). It is also noteworthy that the almost fivefold simultaneous rise of the F_Σ was found, revealing a significant role of twinning in the occurrence of static recrystallization. Judging by the changes in the grain boundary spectra (Figs. 2e-h and 3, and Tab. 1), formation and development of annealing twins were the character for HDEP structures up to completeness of recrystallization at $K_j = 6.8\times10^4$ A^2s/mm^4.

With further increase in impulse capacity to 8.1×10^4 A^2s/mm^4 the weaker decreased hardness (Fig. 1) was mainly conditioned by a faster grain and subgrain coarsening (Figs. 2k,l and Tab. 1), predominantly *via* normal growth, which took place even under extremely short-term heating followed by cooling to room temperature. So, the electric pulsing with high energies resulted in grain coarsening and in the loss of both the work-hardening and the Hall-Petch grain refinement effects. From Fig. 3 it also follows that some impact in Cu softening at this TMT stage was attributed to the changes in grain boundary spectra. Indeed, EBSD data have shown the decrease in fractions of Σ9 twin

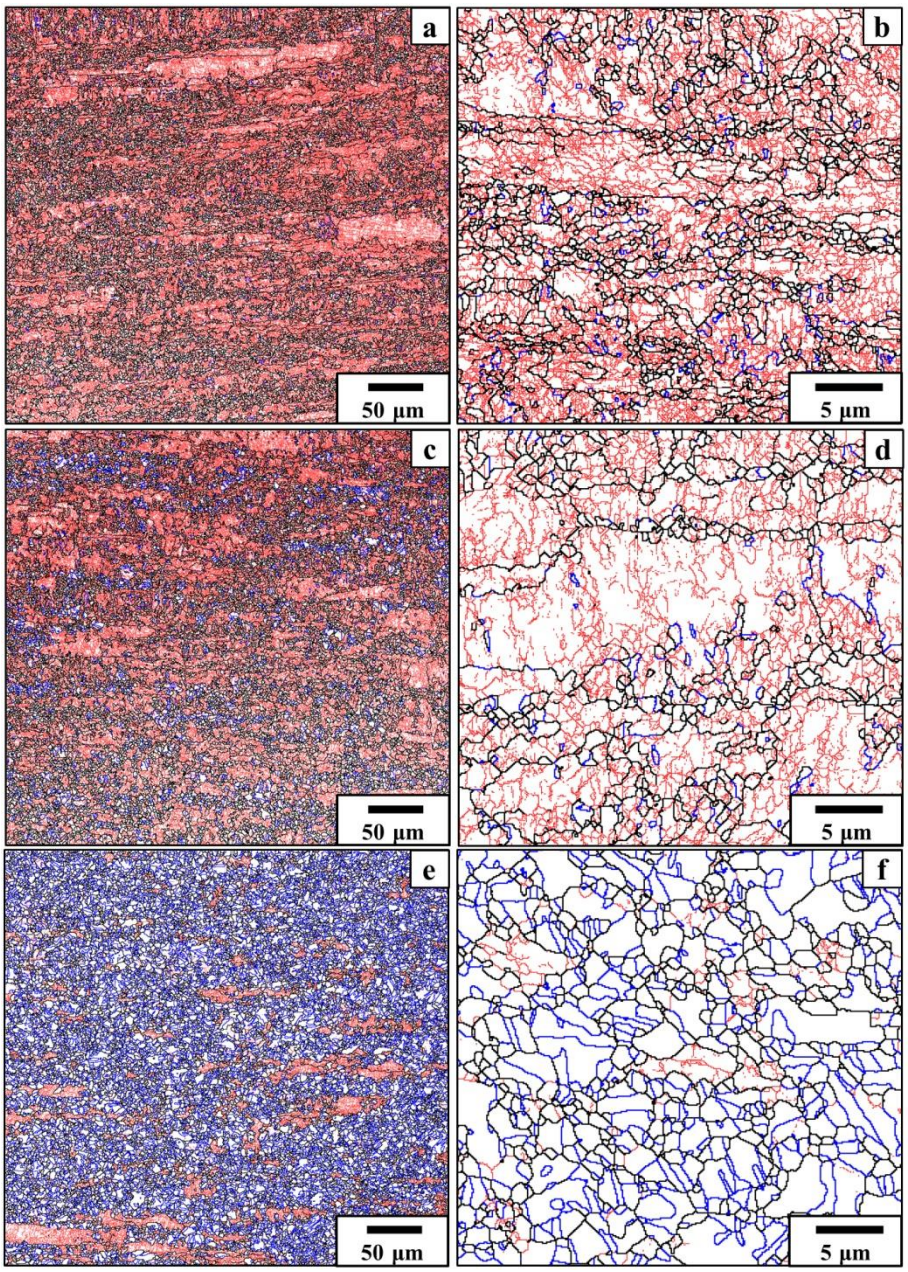

Fig. 2 Grain boundary maps for Cu after CR (a,b) and HDEP with current density of 3.5×10^4 (c,d) and 3.8×10^4 A^2s/mm^4 (e,f). Scanning steps are 500 (a,c,e) and 100 nm (b,d,f). Hereafter red, black and blue lines indicate low-angle, high-angle and twin ($\Sigma3$) boundaries, consequently

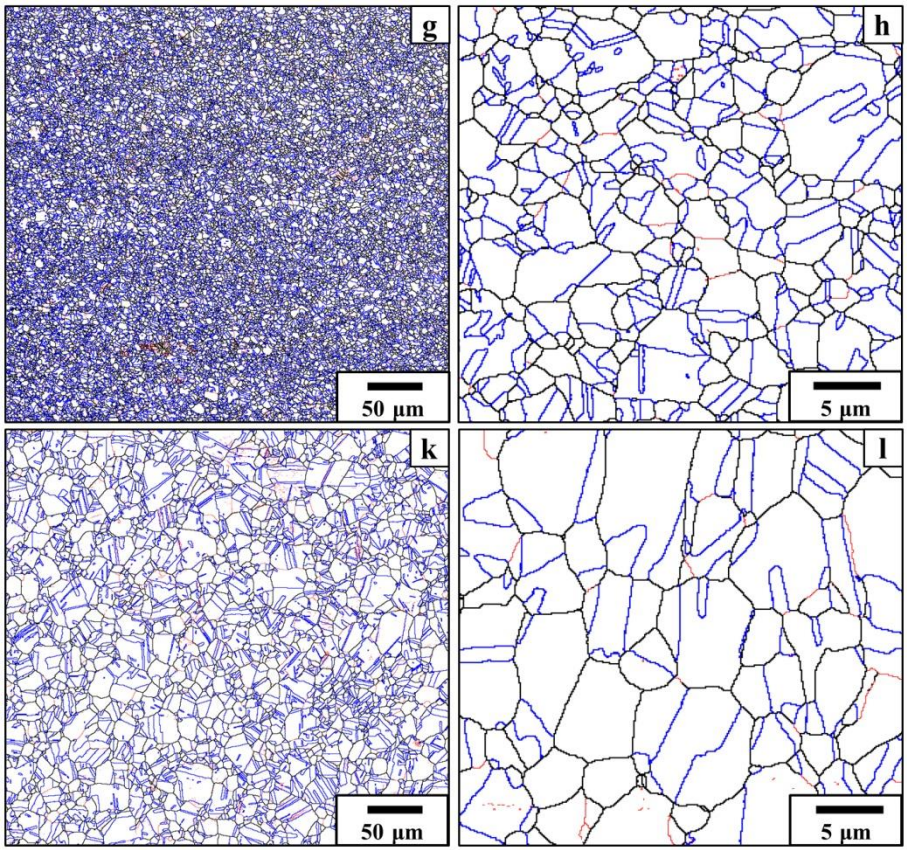

Fig. 2 (continuation) Grain boundary maps for Cu after CR and HDEP with current density of 6.8×10^4 (g,h) and 8.1×10^4 A^2s/mm^4 (k,l).
Scanning step 500 (g,k) and 100 nm (h,l)

boundaries and HABs of 35-55° misorientation angles with increasing the impulse energy. Another interesting finding was observation of a lower coherent domain size with grain coarsening (Tabs. 1 and 2). Virtually, it could be reasoned by the formation of new LABs, dividing new grains, as was found under electric pulsing in [25].

From grain size distributions (Fig. 4) three modes of dependencies, describing the processes of Cu structure changes under the TMT, were evidenced. That is, the first one with a sharp peak at the nanoscale level was found in CR-ed and HDEP-ed states with current density less than the threshold value, being attributed to the formation of deformation structure and its evolution under recovery. The second one was observed in HDEP-ed in an intermediate power range, owing to activation of continuous static recrystallization up to its full completeness. And the third one originated from the normal grain growth at a higher energy of pulsing. Therewith, the first type indicated the absence of any grain coarsening even of the finest grains, the second – the grain coalescence and/or limited grain growth. Under the third one the normal grain growth and twinning changed the dependence, making it linear-like in semi-log coordinates.

Table 1 SEM-EBSD data for Cu after cryorolling and electric pulsing

Condition	K_j, $\times 10^4$ A^{2}s/mm^4	d μm	D μm	F_{rec} %	Θ degree	F_{HABs} %	F_Σ %
CR	-	0.3*	0.7*	15**	17**	33**	2**
HDEP	3.5	0.4	0.9	37	21	42	5
	3.8	0.8	1.0	86	39	79	22
	5.0	0.8	1.3	96	43	88	22
	6.8	1.2	1.3	98	46	93	30
	8.1	1.9	2.5	100	47	90	33

* - scanning step 100 nm, ** - scanning step 500 nm [21]

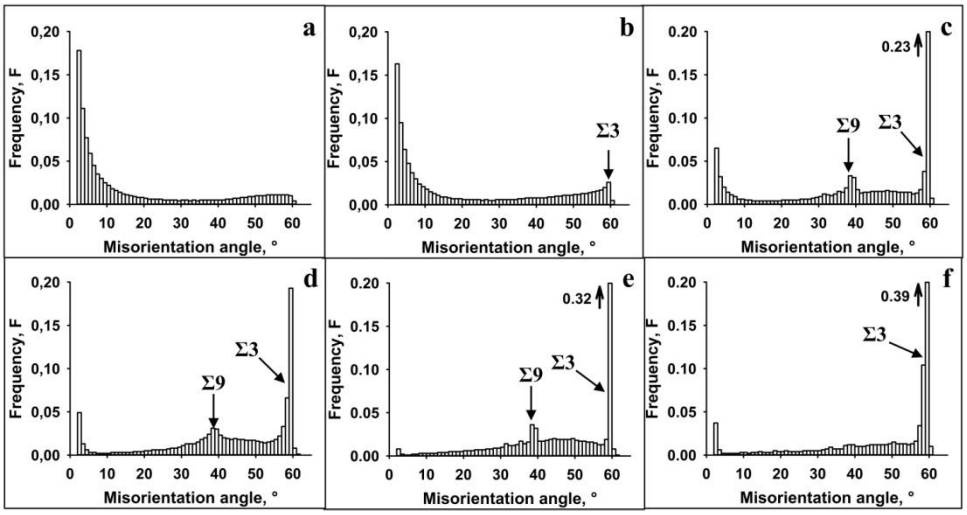

Fig. 3 Boundary spectra in Cu after CR (a) and HDEP with the current density of 3.5×10^4 (b), 3.8×10^4 (c), 5.0×10^4 (d), 6.8×10^4 (e) and 8.1×10^4 A^{2}s/mm^4 (f). Scanning step is 500 nm.

Table 2 X-ray data for Cu after cryorolling and electric pulsing

Condition	K_j, $\times 10^4$ A^{2}s/mm^4	Lattice parameter Å	ρ 10^{14} m^{-2}	D nm	$\langle\varepsilon^{1/2}\rangle$ %
CR	-	3.608±0.001	4.5	57±2	0.186±0.004
HDEP	3.5		3.2	48±2	0.111±0.005
	3.8		0.2	67±4	0.001+0.001
	5.0		0.2	81±3	
	6.8		0.1	100±4	
	8.1		0.2	69±3	

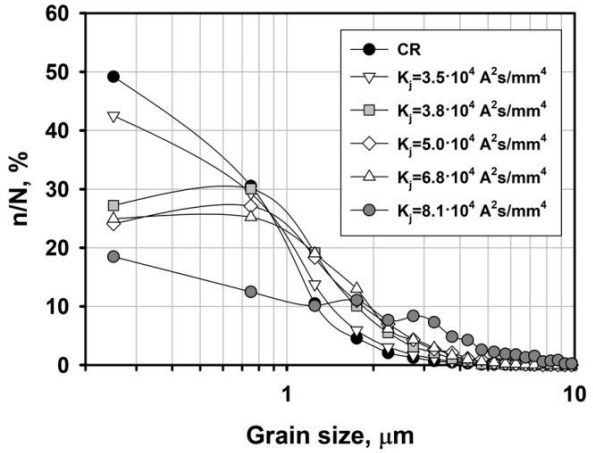

Fig. 4 Grain size distributions in Cu after cryorolling (CR) and pulsing with different current densities (K_j)

All the above discussed Cu structural changes resulted in appropriate texture transformations. The {100}, {110} and {111} pole figures of the CR metal (Fig. 5a) showed rather strong texture with Brass and S (Tab. 3) dominant components, forming a texture different from the rolled Copper-type one found in numerous studies, e.g. [2,26,27]. This may be explained by the fact that the materials, which form the pure metal texture when rolled at room temperature, can develop the alloy-type texture upon straining at lower temperatures [28]. Transition from one type to another is allegedly the result of dislocation cross-slip behavior, which can be suppressed at cryogenic conditions.

Subsequent HDEP with $K_j=3.5\times10^4$ A^2s/mm^4 retained the pole figures (Fig. 5b) and intensities of texture components (Tab. 3) almost as in the CR state. The significant changes started under pulsing with 3.8×10^4 A^2s/mm^4 (Fig. 5c). However, the expected strong Cube-texture, which is usually formed under static recrystallization in conventional work-hardened Cu and attributed to the 40° <111>-orientation relationship with the S-orientation in the rolling texture [28], has not been found in all HDEP-ed conditions. Instead, there were the randomization and weakening of the CR texture accompanied with a near triple decrease in Brass-, twice decrease in S- amid retention of a fewer amount of the Copper-, Cube- and Goss- components (Figs. 5c-e). Besides, the HDEP led to increase in some other components, such as Brass-R (2 3 6) <3 8 5>, Dillamore (4 4 11) <11 11 8>, and especially in the component with the Euler angles (50°;30/60°;0°) (Tab. 3). Judging by the data in [13], such texture transformations could be conditioned by the reaction of the highly deformed metal to the activation of static recrystallization, as was discussed in [12] for furnace annealing of the CR copper. And minimum texture changes with further increasing the HDEP energy (Fig. 5f, Tab. 3) were caused by the completeness of recrystallization with the formation of equilibrium UFG structure with no sign of a drastic grain size increase. Activation of normal grain growth under more powerful pulsing resulted in a slightly intense texture, owing to a higher impact of Brass- and S- components. The latter could also be due to active twinning.

Table 3 Texture components in Cu after cryorolling and electric pulsing

Condition	K_j, $\times 10^4$ A^2s/mm^4	Texture component, %						
		Brass (35;45;90)	Copper (90;35;45)	S (59;37;63)	Brass-R (80;31;35)	Dillamore (50;30;0)	- (55;30;0)	Other
CR	-	35	7	35	8	6	2	7
HDEP	3.5	36	7	37	8	8	4	0
	3.8	11	6	18	9	13	11	32
	5.0	8	8	16	11	13	13	31
	6.8	7	9	18	15	14	14	23
	8.1	11	9	23	15	14	13	15

Thus, the hardening/softening behavior of the copper during cryorolling and subsequent electric pulsing in the present study do not qualitatively differ from the previous ones, reported for copper [3,13], nickel [15,16] aluminum [17] and other pure metals and solid solutions [2,18,19]. Therewith, similarity in their structural behavior was expectable, too. In particular, the phenomenology and nature of the structuring of the Cu under CR found (Figs. 2 and 3) were quite close to those observed in Ni, having the same lattice and close staking fault energy. Indeed, the same type of a structure - a partially recrystallized deformation UFG structure was formed in both metals. The main operating mechanisms of its formation were grain fragmentation (subdivision), dynamic polygonization and recrystallization. Meanwhile, due to the low deformation temperature, these processes resulted in the prevailing formation of low-energy dislocation structures, followed by their transformations into a mixed grain/subgrain structure (Fig. 2 and Tab. 1) with a predominance of dislocation cells misoriented to several degrees and thus, divided mainly by LABs. Like in other materials, the high dislocation densities (Tab. 2) and the extreme refinement of grains and subgrains (Tab. 1) were the main factors that ensured double strengthening of copper (Fig. 1).

Basing on the data presented, one can also conclude that, as in the case of continuous static recrystallization, which is usually observed under furnace annealing of SPD-ed metals [29,30], at the HDEP with energies below the "threshold" K_j value the strain-induced boundaries were gradually transformed to more equilibrium ones under control of static recovery. In the K_j range of 3.5×10^4 - 6.8×10^4 A^2s/mm^4 the main process of structure evolution was *in-situ* recrystallization with limited grain-boundary migration, accompanied with a gradual "transition" to normal grain growth. A sharp drop in hardness at the beginning of this interval, on the one hand, could be caused by fast growth of fine grains formed prior the HDEP. On the other hand, new in-situ formed grains with more equilibrium boundaries acquired a similar ability, limiting grain growth. In both cases, the growth of crystallites was conditioned by a high level of the stored energy and inhomogeneity of the deformation structure. With the amount of pulse energy introduced exceeding the threshold level, the recovery intensively "released" most crystallites from defects and ensured their ability to grow (coalescence), while part of them was still "occupied" by dislocations and underwent polygonization or twinning. At the same time the grain growth was a consequence of restructuring and migration of boundaries, which absorbed defects, and reduced energy of a system and hardness of a material.

It should be noted the high impact of twinning in recrystallization of CR copper and nickel under HDEP. This phenomenon requires special discussion over the frame of the

present paper, as some other points of effectiveness of the TMT studied.

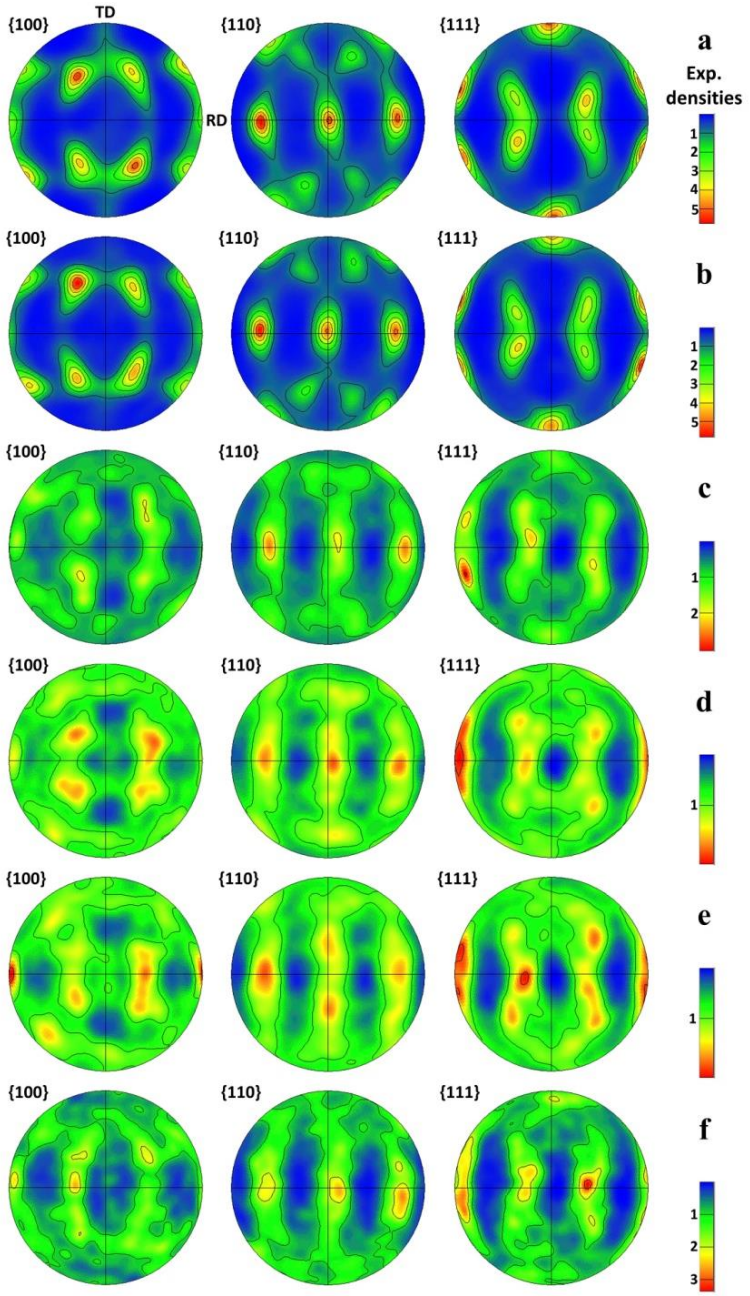

Fig. 5 Pole figures for Cu after cryorolling (a) and further pulsing with current density of 3.5×10^4 (b), 3.8×10^4 (c), 5.0×10^4 (d), 6.8×10^4 (e) and 8.1×10^4 A^2s/mm^4 (f)

4. CONCLUSIONS

Single electric pulse processing of preliminary cryorolled fine-grain copper having highly work-hardened nanostructure with crystallite size of about 300 nm, 30% of HABs fraction and intense rolling texture with Brass and S dominant components, carried out with a current densities below the "threshold" value of $K_j = 3.5\times10^4$ A^2s/mm^4, led mainly to the occurrence of static recovery. This resulted in a more homogeneous and equilibrium structure with minimum changes in texture and structure parameters, as well as in hardness close to that after cryorolling.

Exceeding the K_j "threshold" level was accompanied by a transition to in-situ continuous static recrystallization with limited grain boundary migration and a sharp softening of Cu due to the loss of deformation hardening effect upon transformation of the deformation structure into a recrystallized one with a grain size about 1 μm and more random texture. Increasing HDEP energy in the K_j interval from 4×10^4 to about 8×10^4 A^2s/mm^4 led to normal grain growth to 3 μm and an even higher copper softening.

The nature of the processes, realized under cryorolling and electric pulsing of Cu, are similar to those occurring during conventional cold straining and annealing.

The obtained results testify that the combination of cryorolling and HDEP may be quite advisable for processing fine- and ultrafine-grain copper sheets of a wide strength range.

Acknowledgements: *The work was supported by the Russian Ministry of Science and Higher Education through the state research target and performed using the facilities of the shared services center «Structural and Physics-Mechanical Studies of Materials» at the Institute for Metals Superplasticity Problems, RAS.*

REFERENCES

1. GOST 21957-76, 2005, *Cryogenic Technics. Terms and Conditions*, International Standard. Standardinform, Moscow, Russia, 7 p.
2. Humphreys, F.J., Hatherly, M., 2004, *Recrystallization and related annealing phenomena*, Oxford, Great Britain, 658 p.
3. Konkova, T., Mironov, S., Korznikov, A., Semiatin, S.L., 2010, *Microstructural response of pure copper to cryogenic rolling*, Acta Materialia, 58, pp. 5262-5273.
4. Ma, E., 2006, *Eight routes to improve the tensile ductility of bulk nanostructured metals and alloys*, Journal of Materials, 58. pp. 49-53.
5. Shanmugasundaram, T., Murty, B.S., Subramanya Sarma, V., 2006, *Development of ultrafine grained high strength Al–Cu alloy by cryorolling*, Scripta Materialia, 54, pp. 2013-2017.
6. Krymskiy, S., Sitdikov, O., Avtokratova, E., Markushev, M., 2020, *2024 aluminum alloy ultrahigh-strength sheet due to two-level nanostructuring under cryorolling and heat treatment*, Transactions of Nonferrous Metals Society of China (English Edition), 30, pp. 14-26.
7. Samigullina, A.A., Mukhametgalina, A.A., Sergeyev, S.N., Zhilyaev, A.P., Nazarov, A.A., Zagidullina, Yu.R., Parkhimovich, N.Yu., Rubanik, V.V., Tsarenko, Yu.V., 2018, *Microstructure changes in ultrafine-grained nickel processed by high pressure torsion under ultrasonic treatment*, Ultrasonics, 82, pp. 313–321.
8. Samigullina, A.A., Mukhametgalina, A.A., Nazarov, A.A., Parkhimovich, N.Yu., Zhilyaev, A.P., Tsarenko, Yu.V., Rubanik, V.V., 2018, *Influence of ultrasound on the structure and properties of nickel processed by equal-channel angular pressing*, IOP Conf. Series: Materials Science and Engineering 447, 012017.

9. Laketić, E.S., Rakin, M., Momčilović, M., Ciganović, J., Veljović, Đ., Cvijović-Alagić, I., 2021, *Influence of laser irradiation parameters on the ultrafine-grained Ti45Nb alloy surface characteristics*, Surface and Coatings Technology, 418, 127255.
10. Sarma, V.S., Wang, J., Jian, W.W., Kauffmann, A., Conrad, H., Freudenberger, J., Zhu, Y.T., 2010, *Role of stacking fault energy in strengthening due to cryo-deformation of FCC metals*, Materials Science and Engineering A, 527, pp. 7624-7630.
11. Voronova, L., Degtyarev, M., Chashchukhina, T., Gapontseva, T., Pilyugin, V., 2018, *Formation and Stability of Ultrafine Structure of Commercial Purity Copper Deformed at 80 K*, Letters on Materials, 8, pp. 424-428.
12. Konkova, T., Mironov, S., Korznikov, A.V., Korznikova, G., Myshlyaev, M.M., Semiatin, S.L., 2016, *Grain growth during annealing of cryogenically-rolled Cu-30Zn brass*, Journal of Alloys and Compounds, 666, pp. 170-177.
13. Konkova, T., Valeev, I., Mironov, S., Korznikov, A., Myshlyaev, M.M., Semiatin, S.L., 2014, *Effect of electric-current pulses on grain-structure evolution in cryogenically rolled copper*, Journal of Materials Research, 29, pp. 2727-2737.
14. Konkova, T., Valeev, I., Mironov, S., Korznikov, A., Korznikova, G., Myshlyaev, M.M., Semiatin, S.L., 2016, *Microstructure response of cryogenically-rolled Cu-30Zn brass to electric-current pulsing*, Journal of Alloys and Compounds, 659, pp. 184-192.
15. Valeev, I.Sh., Valeeva, A.Kh., Ilyasov, R.R., Sitdikov, O.Sh., Markushev, M.V., 2019, *Structure and hardness of cold-rolled nickel after single and multiple electric pulse treatment*, Letters on Materials, 9, pp. 447-450.
16. Ilyasov, R.R., Valeeva, A.Kh., Valeev, I.Sh., Sitdikov, O.Sh., Markushev, M.V., 2020, *Effect of electric pulse treatment on the structure and hardness of nickel deformed at room and liquid nitrogen temperatures*, IOP Conf. Series: Materials Science and Engineering, 1008, pp. 012006 (1-6).
17. Valeev, I.S., Valeeva, A.K., Ilyasov, R.R., Avtokratova, E.V., Krymskiy, S.V., Sitdikov, O.S., Markushev, M.V., 2021, *Influence of electric pulse treatment on structure and hardness of cryorolled aluminum*, Letters on Materials, 11, pp. 351-356.
18. Baranov, Yu.V., Troitskiy, O.A., Avraamov, Yu.S., Shlyapin, A.D., 2001, *Physical basics of electro-impulse and electro-plastic treatments and new materials*, Moscow, Russia, 844 p. (in Russian).
19. Liang, Ch.-L., Lin, K.-L., 2018, *The microstructure and property variations of metals induced by electric current treatment: A review*, Materials Characterization, 145, pp. 545-555.
20. Dobatkin, S.V., Salishchev, G.A., Kuznetsov, A.A., Kon'kova, T.N., 2007, *Submicrocristalline structure in copper after different severe plastic deformation schemes*, Materials Science Forum, 558-559, pp. 189–194.
21. Markushev, M.V., Ilyasov, R.R., Krymskiy, S.V., Valeev, I.S., Sitdikov, O.S., 2021, *Structure and strength of fine-grain copper after cryorolling and single electro-pulsing of different capacity*, Letters on Materials, 11, pp. 491-496.
22. Nugmanov, D.R., Sitdikov O.Sh., Markushev, M.V., 2013, *On the comparison of texture data obtained by X-ray diffraction and EBSD analysis of a fine-grained magnesium alloy*, Prospective Materials, S15, pp. 101-105 (in Russian).
23. Humphreys, F.J., 2004, *Characterization of fine-scale microstructures by electron backscatter diffraction (EBSD)*, Scripta Materialia, 51, pp. 771-776.
24. Nowak, W.J., Ochał, K., Filip, R., Wierzba, B., 2021, *The analysis of the residual stress evolution during cycling oxidation of the Ni-base superalloys at high temperature*, Tehnički vjesnik, 28, pp. 540-547.
25. Yan, J., Li, W., Liu, H., Shen, Y., 2019, *Reversion of sub-boundaries into dense dislocations in aluminum by electric pulsing treatment*, Scripta Materialia, 167, pp. 86-90.
26. Vadlamani, S.S., Eickemeyer, J., Schultz, L., Holzapfel, B., 2007, *Rolling and recrystallisation textures in Cu–Al, Cu–Mn and Cu–Ni alloys*, Journal of Materials Science, 42, pp. 7586–7591.
27. Kestens, L.A.I., Pirgazi, H., 2016, *Texture formation in metal alloys with cubic crystal structures*, Materials Science and Technology, 32, pp. 1303-1315.
28. Kallend, J.S., Davies, G.J., 1972, *The development of texture in copper and copper-zinc alloys*, Texture, 1, pp. 51-69.
29. Kobayashi, C., Sakai, T., Belyakov, A., Miura, H., 2007, *Ultrafine grain development in copper during multidirectional forging at 195 K*, Philosophical Magazine Letters, 87, pp. 751-766.
30. Belyakov, A., Sakai, T., Miura, H., Kaibyshev, R., Tsuzaki, K., 2002, *Continuous recrystallization in austenitic stainless steel after large strain deformation*, Acta Materialia, 50, pp. 1547-1557.